J Mater Sci (2010) 45:2239–2245
DOI 10.1007/s10853-009-4119-y

HTC2009

Parametric study for dewetted Bridgman method: crystal–crucible gap dependence on the Bond and Laplace numbers and on contact angle

Simona Epure · Thierry Duffar · Liliana Braescu

Received: 30 May 2009 / Accepted: 9 December 2009 / Published online: 29 December 2009

Abstract In order to analyze the dependence of the crystal-crucible gap on the *Bo* and *La* numbers, a parametric study has been performed for two different cases: the sum of the contact angle (θ_c) and the growth angle (α_e) is smaller or larger then 180°. The limit regimes of the main parameters ($La \to -\infty$, $La \to +\infty$, $Bo \to +\infty$, $Bo \to 0$) of the problem were first studied. Then the non-dimensional Laplace equation has been solved numerically in the axisymmetric case for various values of the parameters and the results are presented as graphical plots. It is shown that the main variations of the gap thickness are localized in the intermediary regimes. Another interesting point is that the gap thickness ($\tilde{e}$) shows a maximum when the *Bo* and *La* numbers are varied. For growing crystals with a uniform radius, since, by definition, the sensitivity to small variations in the relevant parameter is minimal at the maximum, it is advisable to work at the parameter values which yield a maximum gap size.

Introduction

"Dewetting" is a phenomenon by which a solid crystal grows from its melt without contact with the crucible wall, thanks to the stability of a small liquid meniscus for creating a gap between the crystal and the crucible walls [1]. This phenomenon was first obtained spontaneously, in space experiments during the Bridgman solidification of InSb performed on the Skylab-NASA mission-1974 [2, 3]. Numerous other Bridgman crystal growth experiments in space show the same behavior [4]. One of the immediate consequences of this phenomenon is the drastic improvement of the crystal quality.

The phenomenon was later reproduced on the Earth [5, 6] with also an improvement of the crystal quality. On the ground, the dewetting has been obtained by introducing a gas pressure into the crucible with the aim to counteract the hydrostatic pressure and detach the solid away from the crucible wall. This method reproduces artificially the microgravity condition.

The series of experiments performed by Sylla [7] permitted to validate a number of hypotheses, including the existence of the liquid meniscus and its control by manipulating the gas pressure in the ampoule which generally leads to the formation of a constant gap thickness (e) between the solid crystal and the inner crucible walls.

On the physical point of view, the dewetting phenomenon is governed by the Young–Laplace equation through the Bond (*Bo*) and Laplace (*La*) adimensional numbers. Other main parameters identified to enhance the dewetting occurrence are the crucible material and the wetting properties of the melt [8].

Dewetting during Vertical Bridgman growth refers to a physical phenomenon that is strictly defined and applied according to the following criteria:

- The studied materials are pure, doped, or compounds semiconductors.
- The growth procedure is based on the classical Vertical Bridgman technique.
- The existence of a narrow and constant gap (a few micrometers) along several millimeters or centimeters should be achieved.

S. Epure (✉) · L. Braescu
Computer Science Department, West University of Timisoara, 300223 Timisoara, Romania
e-mail: simona_epure7@yahoo.com

S. Epure · T. Duffar
SIMaP-EPM, BP 75, 38402 Saint Martin d'Heres, France

– The crystal surface morphology is different from that of the crucible walls.

In practice, two different cases, $\theta_c + \alpha_e < 180°$ and $\theta_c + \alpha_e \geq 180°$, should be considered, as they lead to different behavior. On the physical point of view, the first case corresponds to the values of Young wetting angles, and the other case corresponds to high contact angles due to gas pollution, oxidation, roughness [7, 8]. They imply different mathematical treatments of the analytical study of the equations [9] and, on the capillary stability point of view, the first case leads to unstable growth and the second one to stable growth [5, 10, 11]. For the unstable cases, it is therefore necessary to introduce an external control device in order to get a crystal with constant radius. Attempts have been made in order to grow crystals in the unstable cases; they use absolute [12] or differential [5] pressure controllers in order to control the difference of pressures between the cold and hot parts of the liquid. A variant simply controls the gas pressure difference by adjusting their temperatures [6].

From sessile drop measurements [13], it is known that the values of the contact angle of the III–V, II–VI, and *Ge* materials increase, respectively, with the following crucible materials: SiO_2, C, BN, and p-BN. Therefore, the experiments carried out on the ground using p-BN crucible material led to the dewetting. Values of the apparent contact angle, higher than 170°, were presented by Palosz et al. [12] for Ge on p-BN. Single crystals of CdTe, Ge, $Ge_{1-x}Si_x$, GaSb, and InSb were grown, thanks to a total dewetting.

Another critical wetting parameter is the growth angle (α_e) that corresponds to the contact angle (θ_c) of a melt on its own solid under dynamic growth condition [14]. Except for InP, the growth angle values of semiconductor melts are between 0° and 30°.

The main purpose of this article is to describe the dependence of the crystal-crucible gap thickness on these relevant parameters which enhance the dewetting occurrence on the Earth.

In order to analyze this dependence, a parametric study has been performed starting from the Young–Laplace equation of a capillary surface written in agreement with the configuration described in Fig. 1:

$$\frac{\frac{d^2z}{dr^2}}{\left[1+\left(\frac{dz}{dr}\right)^2\right]^{3/2}} + \frac{\frac{1}{r}\cdot\frac{dz}{dr}}{\left[1+\left(\frac{dz}{dr}\right)^2\right]^{1/2}} = \frac{\rho_l g(H_m - z) - \Delta p}{\gamma} + \frac{2}{b} \quad (1)$$

where $\Delta p = p_{cold} - p_{hot}$ represents the pressure difference between the cold and hot sides of the sample, θ_c the contact angle, H_m the height of the melt column situated above the top of the meniscus, ρ_l the density of the liquid, g the gravitational acceleration, γ the surface tension of the melt, r the radial coordinate, and the term $2/b$ is due to the curvature at the top. It is important to underline that for crucibles with a reasonable practical radius (larger than the melt capillary constant), the curvature of the upper liquid-free surface is very small in gravity conditions, and hence can be neglected [10].

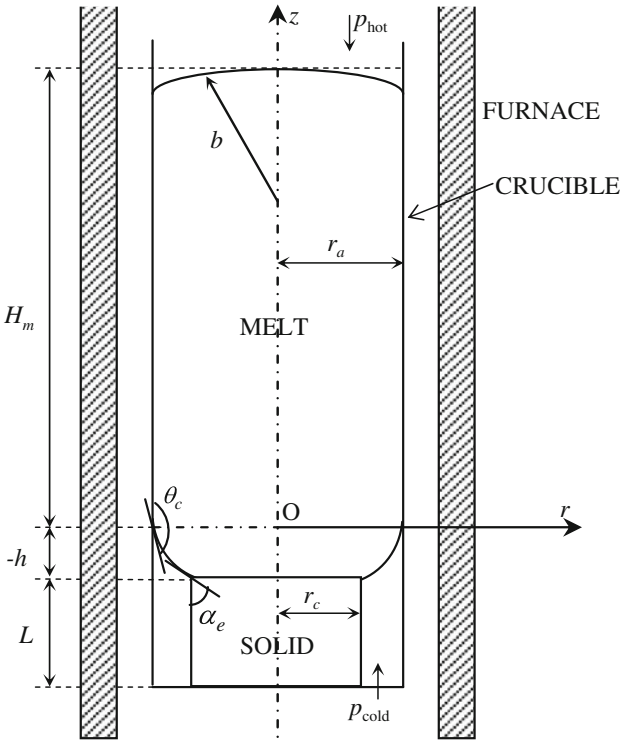

Fig. 1 Schematic dewetted Bridgman crystal growth technique

Procedure and results

Dimensionless Young–Laplace's equation

Introducing the following dimensionless parameters with the ampoule radius r_a, the characteristic dimension of the problem:

$$\tilde{r} = \frac{r}{r_a}; \quad \tilde{H}_m = \frac{H_m}{r_a}; \quad \tilde{z} = \frac{z}{r_a}; \quad \tilde{e} = \frac{e}{r_a} \quad (2)$$

leads to:

$$\frac{dz}{dr} = \frac{d(\tilde{z}\cdot r_a)}{d(\tilde{r}\cdot r_a)} = \frac{d\tilde{z}}{d\tilde{r}};$$

$$\frac{d^2z}{dr^2} = \frac{d}{dr}\left(\frac{dz}{dr}\right) = \frac{1}{r_a}\frac{d}{d\tilde{r}}\left(\frac{d\tilde{z}}{d\tilde{r}}\right) = \frac{1}{r_a}\frac{d^2\tilde{z}}{d\tilde{r}^2}$$

the dimensionless form of Young–Laplace's equation has been obtained:

$$\frac{d^2\tilde{z}}{d\tilde{r}^2} = \left[Bo \cdot \left(\tilde{H}_m - \tilde{z}\right) - La\right] \cdot \left[1 + \left(\frac{d\tilde{z}}{d\tilde{r}}\right)^2\right]^{3/2} - \frac{1}{\tilde{r}}\left[1 + \left(\frac{d\tilde{z}}{d\tilde{r}}\right)^2\right] \cdot \frac{d\tilde{z}}{d\tilde{r}} \quad (3)$$

where $Bo = \frac{\rho_l \cdot g \cdot r_a^2}{\gamma}$ represents the non-dimensional Bond number and $La = \frac{\Delta p \cdot r_a}{\gamma}$ represents the non-dimensional Laplace number.

Taking into account that:

$$\frac{dz}{dr} = \tan\phi \overset{\phi \to \tilde{\phi}}{\Rightarrow} \frac{d\tilde{z}}{d\tilde{r}} = \tan\tilde{\phi}$$
$$\frac{d^2\tilde{z}}{d\tilde{r}^2} = \frac{d}{d\tilde{r}}\left(\frac{d\tilde{z}}{d\tilde{r}}\right) = \frac{d}{d\tilde{r}}\left(\tan\tilde{\phi}\right) = \frac{1}{\cos^2\tilde{\phi}}\frac{d\tilde{\phi}}{d\tilde{r}} = \left(1 + \tan^2\tilde{\phi}\right)\frac{d\tilde{\phi}}{d\tilde{r}} \quad (4)$$

the following dimensionless form of Young–Laplace's equation is obtained:

$$\frac{d\tilde{\phi}}{d\tilde{r}} = \left[Bo \cdot \left(\tilde{H}_m - \tilde{z}\right) - La\right] \cdot \frac{1}{\cos\tilde{\phi}} - \frac{1}{\tilde{r}} \cdot \tan\tilde{\phi}. \quad (5)$$

Therefore, Eq. 3 is transformed into the following non-linear system of two differential equations [9]:

$$\begin{cases} \dfrac{d\tilde{z}}{d\tilde{r}} = \tan\tilde{\phi} \\ \dfrac{d\tilde{\phi}}{d\tilde{r}} = \left[Bo \cdot \left(\tilde{H}_m - \tilde{z}\right) - La\right] \cdot \dfrac{1}{\cos\tilde{\phi}} - \dfrac{1}{\tilde{r}} \cdot \tan\tilde{\phi} \end{cases} \quad (6)$$

with the corresponding boundary condition:

$$\tilde{z}(1) = 0, \quad \tilde{\phi}(1) = \theta_c - \frac{\pi}{2}; \quad \theta_c \in \left(\frac{\pi}{2}, \pi\right) \quad (7)$$

The mathematical model given by Eqs. 6 and 7 is very useful for obtaining information concerning the meniscus behavior (shape, monotony, achievement of the growth angle, etc.). Once the meniscus shape (global convex, global concave, convexo–concave, or concave–convex, see [9, 15]) is obtained, *the growth angle criterion* should be imposed. The growth angle defines the point, on the meniscus line, where the meniscus joins the solid–liquid interface [9, 15]. This condition is expressed as follows:

$$\tilde{\phi}\big|_{\tilde{r}=\tilde{r}_c} = \frac{\pi}{2} - \alpha_e,$$

where $\tilde{r}_c$ represents the non-dimensional crystal radius.

According to [10, 11], the convex meniscus is capillary stable and then only the achievements of the growth angle on the convex part of the menisci were considered. It should be mentioned that the thermal effects were neglected which is fully valid under microgravity conditions ($Bo = 0$, cf. [5, 10, 11]) but would deserve a more complete study on the ground. Only the case where the local thermal field close to the crystal–liquid–meniscus triple line makes dewetting possible [16, 17] was considered here.

Numerical results

In order to study the dependence of the crystal–crucible gap ($\tilde{e} = 1 - \tilde{r}_c$) on the *Bo* and *La* numbers, a parametric study has been performed for the two different cases: $\theta_c + \alpha_e < 180°$ and $\theta_c + \alpha_e \geq 180°$. The limit regimes of the main parameters ($La \to -\infty$, $La \to +\infty$, $Bo \to +\infty$, $Bo \to 0$) which enhance the dewetting occurrence were first studied. Then the Cauchy problem (6) and (7) have been solved numerically using the *adaptive* fourth-order Runge–Kutta method [9] for various values of the parameters. Once all the solutions of the system are computed, the evolution of the crystal–crucible gap thickness can be presented as graphical plots.

The dependence of the dimensionless gap thickness on the Bond number, for different values of *La*, in the cases $\theta_c + \alpha_e < 180°$ and, respectively, $\theta_c + \alpha_e \geq 180°$ is shown in Figs. 2 and 3.

The dependence of the dimensionless gap thickness on the Laplace number is illustrated in Figs. 4 and 5 for different values of *Bo*, in the cases $\theta_c + \alpha_e < 180°$ and $\theta_c + \alpha_e \geq 180°$.

It can be observed that the crystal–crucible gap thickness shows a maximum (see Figs. 2–5b–e) when the *Bo* and *La* numbers are varied. Maximum of the gap thickness decreases when the *Bo* and *La* increase.

In the case $\theta_c + \alpha_e < 180°$, most of the menisci are globally concave and the gap cannot reach high values. As already noted, this is a capillary unstable configuration. The case $\theta_c + \alpha_e \geq 180°$ means a convex meniscus that usually gives larger gap thicknesses and a good stability of the process.

In Fig. 6, the crystal–crucible gap thickness is plotted versus the contact angle and, respectively, the growth angle. Thus, an increase in the contact angle leads to a decrease in the maximum gap thickness and increasing the growth angle the maximum gap thickness will increase too.

Discussion

An interesting point is that the gap thickness shows a maximum when the *La* number is varied, which means that a small variation of pressure difference between the hot and cold sides of the crucible ($La = \Delta p \cdot r_a/\gamma$) has a limited effect on the gap thickness:

$$\frac{\partial \tilde{e}}{\partial La} = 0.$$

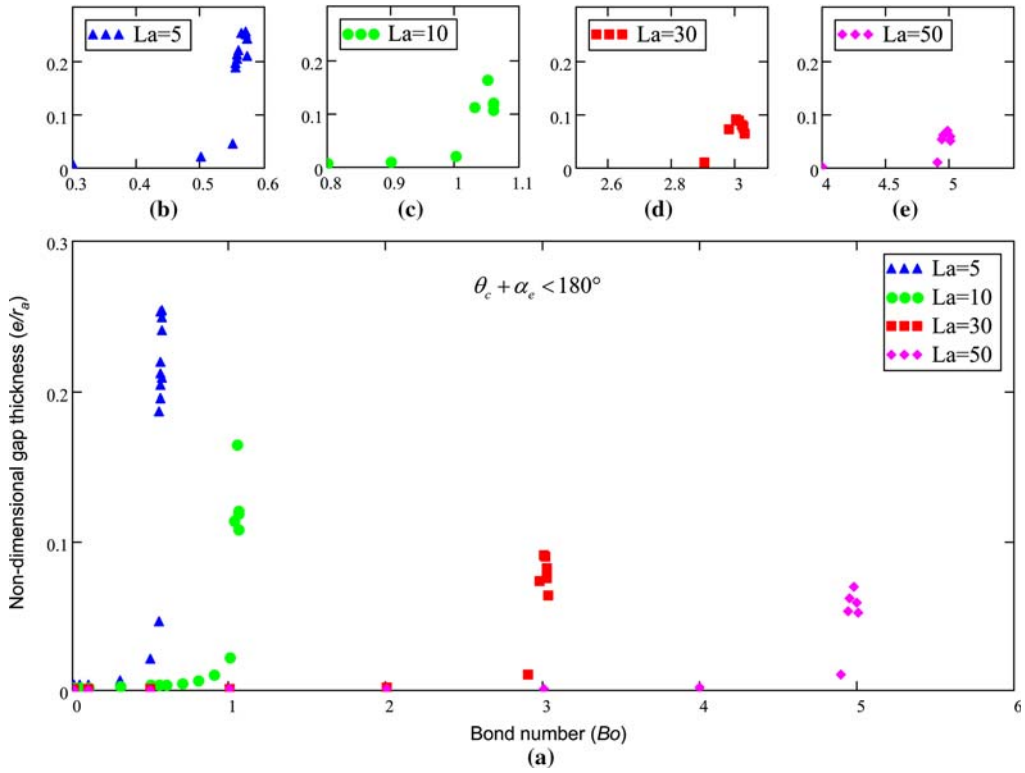

Fig. 2 Non-dimensional gap thickness as function of Bond number for the case $\theta_c + \alpha_e = 164° + 11° < 180°$

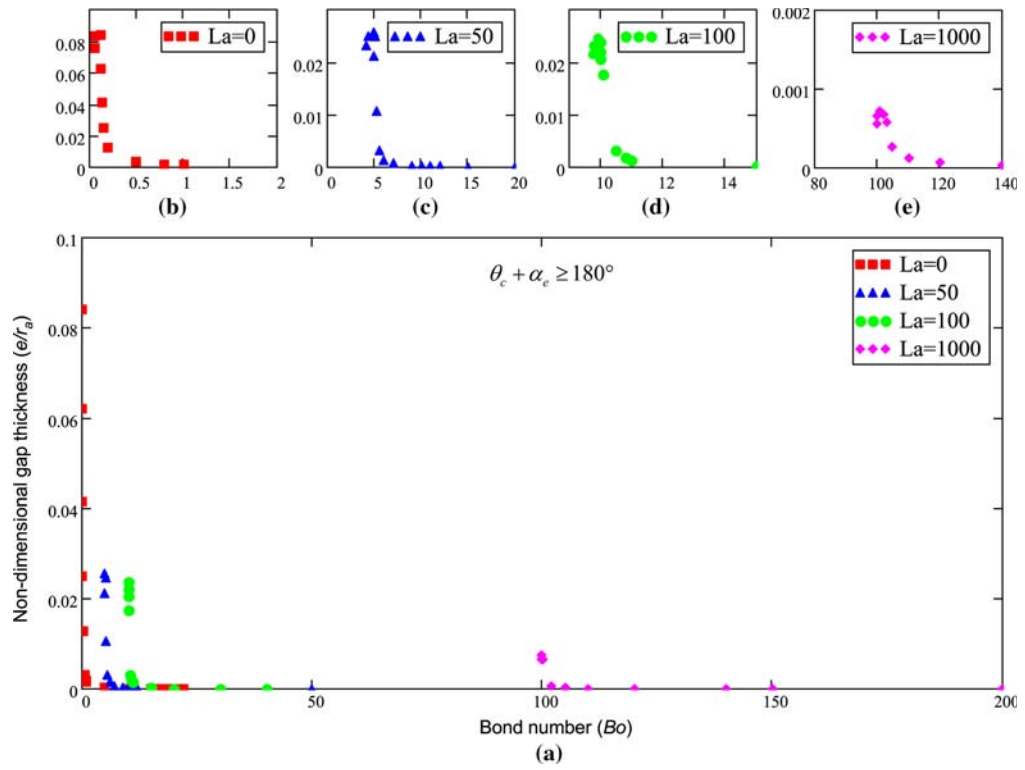

Fig. 3 Non-dimensional gap thickness as function of Bond number for the case $\theta_c + \alpha_e = 174° + 11° > 180°$

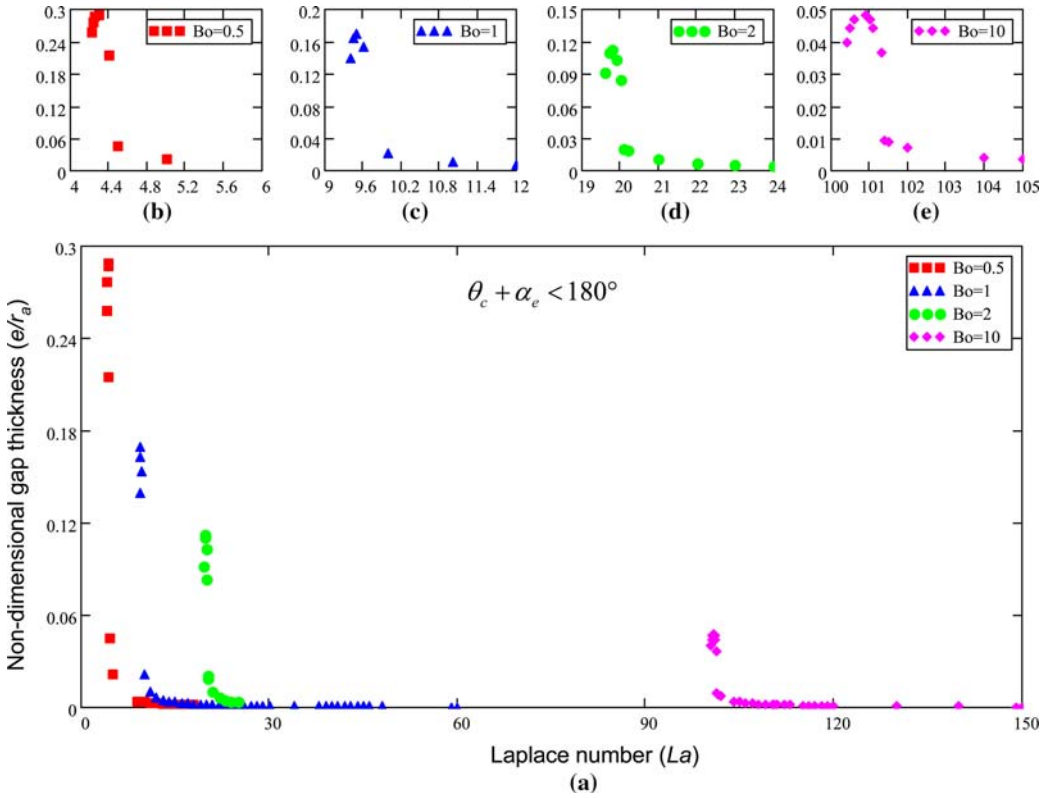

Fig. 4 Non-dimensional gap thickness as function of Laplace number for the case $\theta_c + \alpha_e = 164° + 11° < 180°$

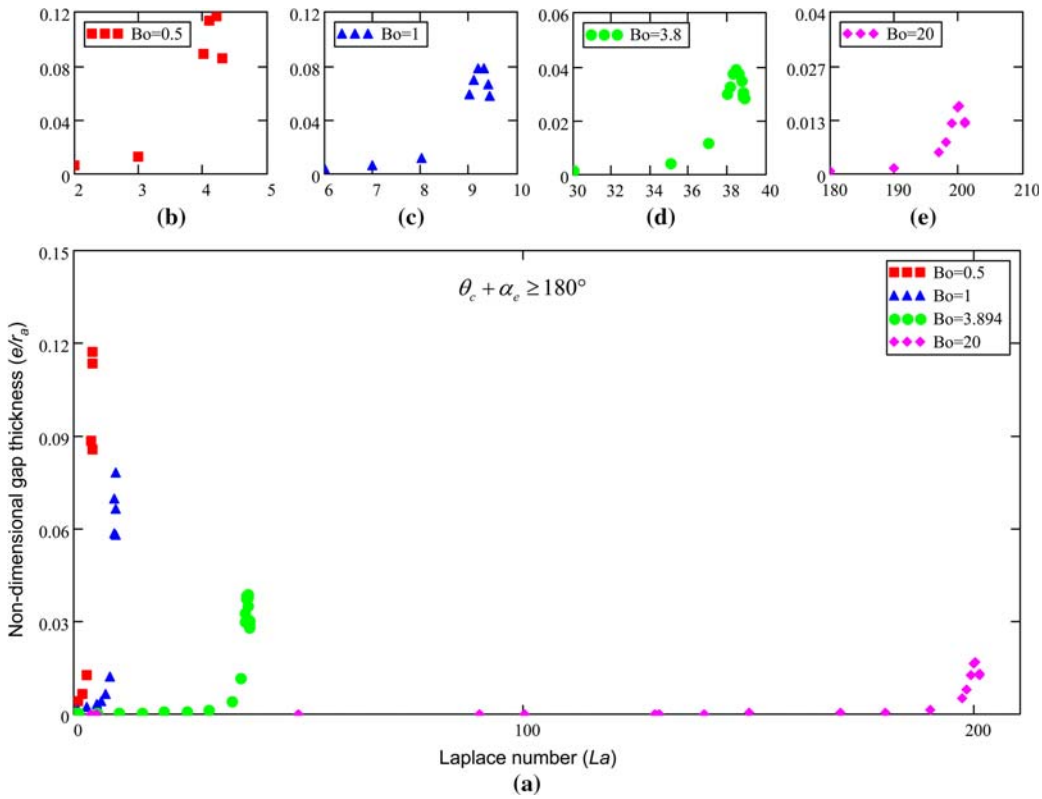

Fig. 5 Non-dimensional gap thickness as function of Laplace number for the case $\theta_c + \alpha_e = 174° + 11° > 180°$

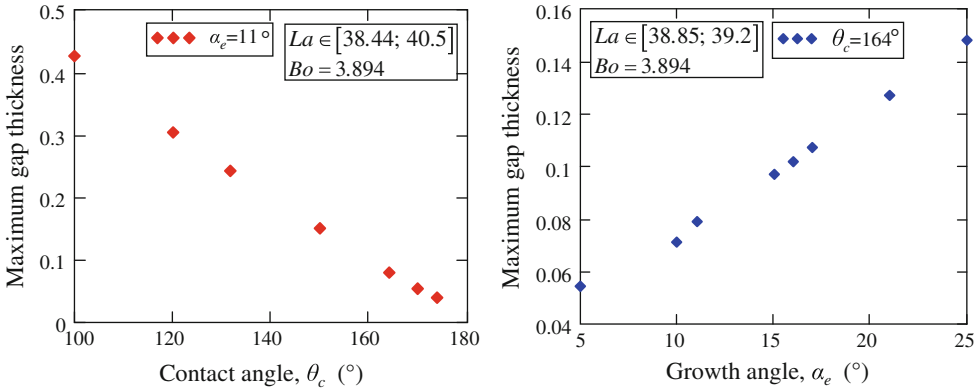

Fig. 6 Non-dimensional maximum gap thickness as function of the contact angle and growth angle

For both cases, $\theta_c + \alpha_e < 180°$ and $\theta_c + \alpha_e \geq 180°$, this maximum appears in the cases where the growth angle is achieved on a convex part of the meniscus, which, for stability reasons, is the preferred practical case [9, 11, 15].

As for growing crystals with a uniform radius, it is important that small variations of the relevant parameters have a low effect on the crystal–crucible gap thickness, the maximal values are preferred for practical growth of crystals.

In Fig. 7, the Laplace number corresponding to the maximum value of the crystal–crucible gap thickness is plotted versus the Bond number for a fixed growth angle $\alpha_e = 11°$ and different values of the contact angle which leads to the cases $\theta_c + \alpha_e < 180°$, $\theta_c + \alpha_e = 180°$, and $\theta_c + \alpha_e \geq 180°$.

The variation of the optimal *La* number with *Bo* number is shown to be linear and practically independent of the value of the wetting and growth angles (see Tables 1 and 2). This means that *La* (the applied gas pressure) does not change practically for various crucible materials. In fact, the main effect of the gas pressure difference is to counteract the hydrostatic pressure which is almost independent of the contact angle.

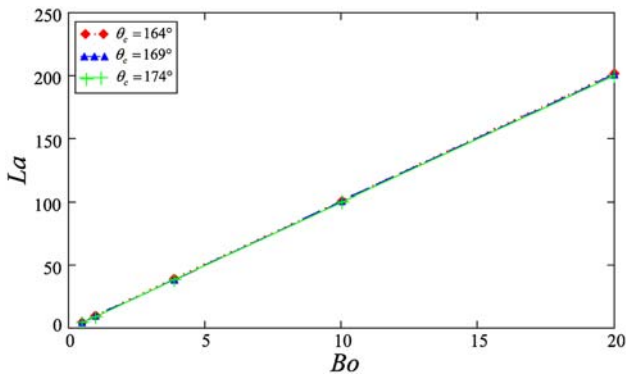

Fig. 7 Optimal Laplace number corresponding to the maximum gap thickness versus Bond number

Table 1 Values of optimal Laplace number corresponding to the maximum gap thickness for different values of Bond number and growth angle $\alpha_e = 11°$

$\alpha_e = 11°$	*La*		
Bo	$\theta_c = 164°$	$\theta_c = 169°$	$\theta_c = 174°$
0.5	4.3	4.24	4.2
1	9.5	9.4	9.3
3.894	39	38.79	38.44
10	100.9	100.5	99.86
20	201.5	200.9	200

Table 2 Values of optimal Laplace number corresponding to the maximum gap thickness for different values of Bond number and contact angle $\theta_c = 164°$

$\theta_c = 164°$	*La*		
Bo	$\alpha_e = 11°$	$\alpha_e = 16°$	$\alpha_e = 21°$
0.5	4.3	4.255	4.21
1	9.5	9.45	9.41
3.894	39	38.9	38.85
10	100.9	100.6	100.5
20	201.5	201.3	201.2

These results give a good understanding of the physics of the dewetting process and are basic reference tools for the practical crystal growers working with a given equipment and given materials and also for the equipment designers.

Acknowledgement The authors are grateful to the European Space Agency (Map-CdTe program) and the *Romanian National University Research Council* (Grant PN II 131/2009-2011) for support of this project.

References

1. Duffar T, Paret-Harter I, Dusserre P (1990) J Cryst Growth 100:171
2. Witt AF, Gatos HC (1974) In: Proceeding of the space processing symposium MSFC, Alabama, NASA M74-5, vol 1, p 275
3. Gatos HC, Witt AF et al (1975) In: Skylab science experiments proceeding symposium, 1974, Sci Technol Series, vol 38, p 7
4. Regel LL, Wilcox WR (1998) Microgravity Sci Technol X1/4:152
5. Duffar T, Dusserre P, Picca F, Lacroix S, Giacometti N (2000) J Cryst Growth 211:434
6. Duffar T, Dusserre P, Giacometti N (2001) J Cryst Growth 223:69
7. Sylla L (2008) PhD Thesis, Institut national Polytechnique de Grenoble (in French)
8. Duffar T, Sylla L (2010) In: Duffar T (ed) Crystal growth processes based on capillarity, chap 6. Wiley-Blackwell, Oxford, UK. ISBN 978-0-470-71244-3
9. Braescu L, Epure S, Duffar T (2010) In: Duffar T (ed) Crystal growth processes based on capillarity, chap 8. Wiley-Blackwell, Oxford, UK. ISBN 978-0-470-71244-3
10. Duffar T, Boiton P, Dusserre P, Abadie J (1997) J Cryst Growth 179:397
11. Epure S, Duffar T, Braescu L (2009) J Cryst Growth. doi: 10.1016/j.jcrysgro.2009.11.050
12. Palosz W, Volz MP, Cobb S, Motakef S, Szofran FR (2005) J Cryst Growth 277:124
13. Harter I, Dusserre P, Duffar T, Nabot JP, Eustathopoulos N (1993) J Cryst Growth 131:157
14. Eustathopoulos N, Drevet B, Brandon S, Virozub A (2010) In: Duffar T (ed) Crystal growth processes based on capillarity, chap 1. Wiley-Blackwell, Oxford, UK. ISBN 978-0-470-71244-3
15. Braescu L (2008) J Colloid Interface Sci 319:309
16. Stelian C, Yeckel A, Derby J (2009) J Cryst Growth 311:2572
17. Stelian C, Volz MP, Derby J (2009) J Cryst Growth 311:3337